Journal of Polymer Research (2019) 26: 88
https://doi.org/10.1007/s10965-019-1746-0

ORIGINAL PAPER

Kinetic and thermodynamic studies of molecularly imprinted polymers for the selective adsorption and specific enantiomeric recognition of D-mandelic acid

T. Sajini[1,2,3] · M. G. Gigimol[2] · Beena Mathew[3]

Received: 20 November 2018 / Accepted: 26 February 2019 / Published online: 12 March 2019

Abstract

In the present article, we fabricated an artificial sorbents of D-mandelic acid (D-MA) on vinyl functionalized multiwalled carbon nanotube (MWCNT) by molecular imprinting technology. Here molecular imprinted polymers (MIPs) were tailored by D-MA as a template molecule on the surface of the vinyl functionalized MWCNT with 4-vinyl pyridine (4-VP) as the functional monomer, ethylene glycol dimethacrylate (EGDMA) as the crosslinking agent and 2,2′-azo-bis-isobutyronitrile (AIBN) as the initiatorvia a thermal polymerization technique. For better evaluation, blank polymer (MWCNT-NIP) was prepared by the same procedure, only without using the template molecule in the polymerization process. To get a better knowledge of the role of MWCNT on chiral recognition, D-MA imprinted and non-imprinted polymers without MWCNT were also prepared and analysed. Fourier transform infrared spectra (FT-IR), X-ray diffraction technique (XRD), Thermogravimetric analysis (TGA), Scanning electron microscopy (SEM) and Transmission electron microscopy (TEM) were used to characterize the composite structure, morphology and determine the grafted MIP quantities in the composite. Selective adsorption and specific chiral recognition of synthesised polymers were examined using the theory of kinetics and thermodynamics. The resulting MWCNT-MIP demonstrated favorable selectivity, good stability and a higher adsorption capacity for the template particle compared to products created by bulk polymerization. The thermodynamic studies revealed that the adsorption was controlled by enthalpy and that MWCNT-MIPs had higher enthalpy and entropy than conventional polymers which contributed to the specific recognition of MWCNT-MIPs. D-MA adsorption on MWCNT-MIP is in good agreement with Langmuir adsorption isotherm and kinetics obey second order rate expression with rate constant $k_2 = 0.1482$ mol^{-1} min^{-1}. Kinetic correlation indicated that there was fast and selective adsorption equilibrium for D-MA molecules in MWCNT-MIPs happen because of the homogenous binding sites of template molecules on the surface of nanotubes.

Keywords D-mandelic acid · Molecular imprinting · Multiwalled carbon nanotube · Binding isotherm · Kinetics · Thermodynamics · Selectivity

✉ Beena Mathew
beenamathew@mgu.ac.in

[1] Research & Post Graduate Department of Chemistry, St Berchmans Autonomous College, Affiliated to Mahatma Gandhi University, Changanassery, Kottayam, Kerala 686101, India

[2] Research & Post Graduate Department of Chemistry, St Thomas College, Affiliated to Mahatma Gandhi University, Pala, Kerala 686574, India

[3] School of Chemical Sciences, Mahatma Gandhi University, Priyadarsini Hills, Kottayam, Kerala 686560, India

Introduction

Molecular imprinting is one of the promising techniques for the fabrication of artificial sorbents of the template molecule on a polymer matrix [1]. The general mode of synthesis of MIPs was depicted in Scheme 1. These polymers possess predetermined selectivity, specificity and high affinity towards the template molecule in which involves arrangement of polymerizable functional monomers around a target molecule [2]. Molecularly imprinted polymers (MIPs) have the ability to specifically distinguish and

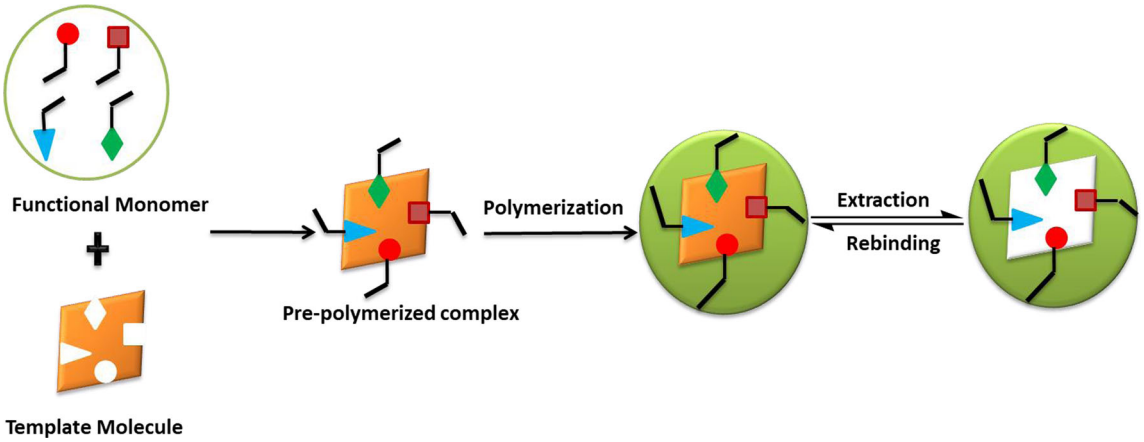

Scheme 1 Schematic representation of molecular imprinting process

separate a particular molecule from other molecules of similar structures [3, 4]. This property makes MIPs applicable in various fields such as in separation and purification of structurally related compounds, catalysis, biosensors, drug delivery, and in biotechnology [5, 6]. Among the various approaches used during the synthesis of MIPs, non-covalent interaction can be considered the best one due to easy removal of template, applicable for a variety of molecules, economical and easy method [7–9]. The ultimate mechanisms for molecular recognition demonstrated by the imprinting effect can be attributed to two processes. They are (a) the pre-organization of complementary functional groups in the polymer by the template and (b) the formation of a shape-selective cavity that is complementary to the template [10].

The role of MIPs in chiral separation of racemic mixtures is most important because the classic techniques are not efficient for these purposes. In the present work we were selecting D-mandelic acid (D-MA) as the template molecule which is a significant chiral analogue of amino acids in the pharmaceutical synthetic industry, and is employed for various application fields such as the treatment of urinary tract infections [11], precursor for the synthesis of cephalosporin and penicillin [12], chiral resolving agent and chiral synthon for the synthesis of anti-tumour and anti-obesity agents [13]. Although many approaches have been used for recognizing MA, designing a simple and efficient system for enantioselective recognizing MA enantiomer is still a challenging task [14, 15]. Development of MIPs using D-MA as target molecule will leads to an efficient chiral separating system in separation science.

The main issues in molecular imprinting technology are its low selectivity, low response towards the target molecule and large template size limitations. Thus many efforts were done to tenacity these problems in past decades [16–18]. One of the techniques is based on the small dimension with extremely high surface-to-volume ratio of nano-imprinting materials, which enable the imprinting technique to generate more effective recognition sites than those obtained by traditional approaches which only use porogens [19–21]. The imprinting of molecular recognition sites at nanostructures has greatly improved the removal of templates and the binding capacities and kinetics of molecular recognition, compared with the traditional imprinted bulky materials [22–24].

Multiwalled carbon nanotubes (MWCNTs) have enjoyed widespread attention because of their high electrical, mechanical and thermal conductivity properties [25–27]. MWCNTs, with extremely large surface area, should be an excellent nominee as the support material in molecular imprinting technology. If the MIPs were prepared onto the surface of MWCNTs, it increases the number of homogeneous binding sites [28–30]. Consequently the binding sites in the outer layer of the composite would improve the accessibility of template molecule and reduce the binding time [31]. In order to get homogeneous MIPs layer on MWCNTs, it is necessary to modify MWCNTs with high density carboxyl functional groups by strong acid treatment [32], subsequently obtain vinyl group functionalized MWCNTs via covalent reaction, then the cross-linker and monomer would couple with the vinyl groups on the surface of MWCNTs, which forming uniform MIPs layer.

In the present study, a novel composite of MIPs with D-mandelic acid as the template molecule was prepared by selective polymerizing MIPs onto the vinyl group functionalized MWCNTs surface. Vinyl group functionalized MWCNTs directed selective polymerization of MIPs by covalent bonds on the MWCNTs surface [16]. For the synthesis of MIPs, compounds with functional groups reciprocal to those of the template are selected as functional monomer and are used to form a framework around the preferred template. Here 4-vinylpyridine (4-VP) was selected as the functional monomer because of its basic functionality and commercial availability which could pre-associate with D-mandelic acid through

several non-covalent processes including electrostatic attraction, hydrogen bonding, and π-π stacking interaction. The resulting MWCNT-MIP demonstrated favorable selectivity, good stability and a higher adsorption capacity for the template molecule compared to products created by bulk polymerization. For evaluation, blank polymers (MWCNT-NIP) were prepared by the same procedure, only without using the template molecule in the polymerization process. To analyse the role of MWCNTs on chiral recognition, D-MA imprinted and non-imprinted polymer without MWCNTs were also prepared.

Experimental

Materials & instruments

D-MA and L-MA with 99% purity were purchased from SRL, Mumbai. MWCNTs were obtained from Reinste Nano Ventures Private Limited, New Delhi, India. Ethylene glycol dimethacrylate (EGDMA) was from Sigma Aldrich. 4-Vinyl pyridine (4-VP), vanillylmandelic acid (VMA) and homovanillic acid (HVA) were from Alfa Acer. The initiator, 2,2′-azo-bis-isobutyronitrile (AIBN) was from Merck. The solvent acetonitrile was analytical grade and purchased from Merck. 4-VP was stabilized with hydroquinone and was destabilized by distillation under reduced pressure.

Fourier Transform Infrared spectrometer 8400 s (DIN 206–72,400), Shimadzu, Japan was used to record FT-IR spectra of samples. The binding studies were carried out on a Shimadzu-UV-vis Spectrophotometer model 2450. For the morphological studies of the polymer samples, Transmission Electron Microscope (TEM) Facility JEOL JEM - 2100 and Scanning Electron Microscope (SEM) – JEOL-JSM-6390A were used. PAN analytic X'PERT PRO was used for the X-ray diffraction studies of polymer. Thermogravimetric analysis (TGA) was conducted on a NETZSCHSTA449C instrument from room temperature to 500 °C in N_2 atmosphere.

Fabrication of vinyl group on the surface of MWCNTs

Carbon nanotubes were found to have great potential applications in various fields such as biosensors and nanobiotechnology. The poor dispersibility and bundling between carbon nanotube tubules are major problem which affected in various applications of carbon nanotube. Surface modification of carbon nanotubes through functionalization process is the way to overcome these disadvantages. For the functionalization of MWCNT (Scheme 2), crude MWCNTs (0.5 g) was added to 60 mL of 70% HNO_3 under sonication for 10 min. Then the mixture was stirred under 85 °C for 16 h. After cooling to room temperature, the mixture was filtered through a 0.22 μm polycarbonate membrane and washed thoroughly with distilled water until the pH value of the filtrate became neutral. The filtered solid was dried under vacuum, obtaining acid-functionalized MWCNTs (MWCNTs-COOH).To get acyl functionalized MWCNTs, MWCNTs-COOH (0.4 g) was suspended in the mixture of 10 mL of sulfoxide chloride ($SOCl_2$) and 30 mL chloroform at 60 °C for 24 h under reflux. The solid was washed by anhydrous tetrahydrofuran (THF) for several times to remove the excess $SOCl_2$ and dried under vacuum to give MWCNTs-COCl. Allyl alcohol (1.16 g), 4-DMAP (0.244 g) and triethylamine (6.06 g) were added to MWCNTs-COCl (0.2 g) in anhydrous THF(30 mL). The mixture was stirred at 60 °C for 24 h and then collected by centrifugation and washed with anhydrous THF. After washing and centrifugation, the resulting solid was dried overnight in a vacuum desiccator, obtaining vinyl group functionalized MWCNTs (MWCNTs-CH=CH_2).

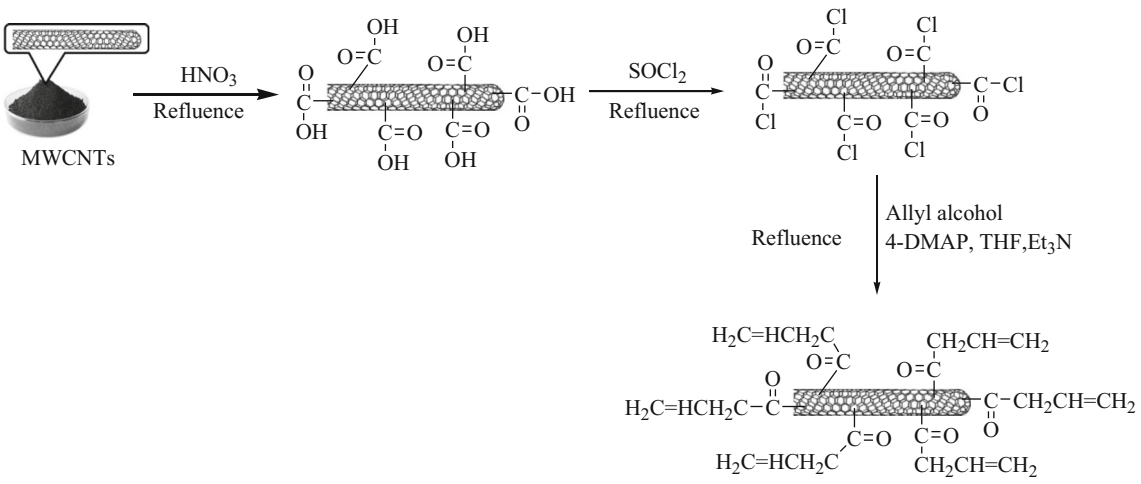

Scheme 2 Schematic representation of synthesis of vinyl functionalized MWCNTs

Synthesis of imprinted and non-imprinted polymer on vinyl functionalized MWCNTs

MIPs with D-MA as a template molecule were prepared by selective polymerizing MIPs onto the vinyl group functionalized MWCNT surface. The mode of synthesis is represented in Scheme 3. MWCNT-CH=CH_2(0.02 g) was added to 30 mL of acetonitrile in a 250 mL round-bottom (RB) flask and purged with N_2 under magnetic stirring. D-MA (0.05 mmol) and 4-VP (0.25 mmol) dissolved in 5 mL of acetonitrile were added to the RB flask and mixed for 30 min to form a complex of template and functional monomer. The initiator AIBN(10 mg) and cross-linker EGDMA (1.25 mmol) were added. The temperature of the pre-polymerized solution was raised to 65 °C, and the reaction was allowed to proceed for 8 h in nitrogen atmosphere. The resulting product was collected by centrifugation and washing thoroughly with ethanol to discard the reagents. The template molecule was eluted by the solvent acetonitrile until no D-MA could be detected by UV-vis. (at 257.5 nm) in the eluent. The obtained polymers were finally rinsed with ethanol to remove the remaining acetonitrile and subsequently ground, dried in vacuum desiccator and sieved to get particles with a size less than 25 μm. For comparison, blank polymers (MWCNT-NIP) were prepared by the same procedure, only without using the template molecule in the polymerization process. D-MA imprinted and non-imprinted polymers without MWCNTs were also prepared.

Adsorption studies

The adsorbed amount of D-MA on each polymer was monitored by a UV-vis. Spectrophotometer at 257.5 nm. For this 10 mg of each polymer were transferred into a tube containing 7.0 mL of acetonitrile solution with specific initial concentrations of D-MA ranging from 0.15 to 0.45 mmol L^{-1}. The binding process was allowed to proceed for about 3 h at 28 °C for the adsorption of D-MA. The mixture was centrifuged at 15000 rpm for 5 min. Finally, the extracted solution was monitored by a UV-vis. Spectrophotometer and the concentration of free D-MA in the supernate was measured. The amount of D-MA adsorbed, Q_e (μmol g^{-1}) onto the polymer was determined according to the following equation

$$Q_e = \frac{(C_i - C_f)V}{m} \quad (1)$$

whereC_i (mg/ml) and C_f(mg/ml) represent the initial and final D-MA solution concentration, respectively. V (ml) is the sample's volume and m(g) is the mass of the polymer. The experiments were carried out in duplicate. Binding capacity can be determined using the equation [33],

$$Binding\ capacity = \frac{C_i - C_f}{C_i} * 100 \quad (2)$$

Adsorption dynamics and kinetics

The experiments for the adsorption kinetics were implemented at three temperatures (291, 301, and 311 K) for 10 to 180 min. The thermodynamic parameters were achieved based on the effect of these temperatures. The time taken for the saturated rebinding specificity was investigated by incubating equal amount of polymer in template solution of known concentration of D-MA at

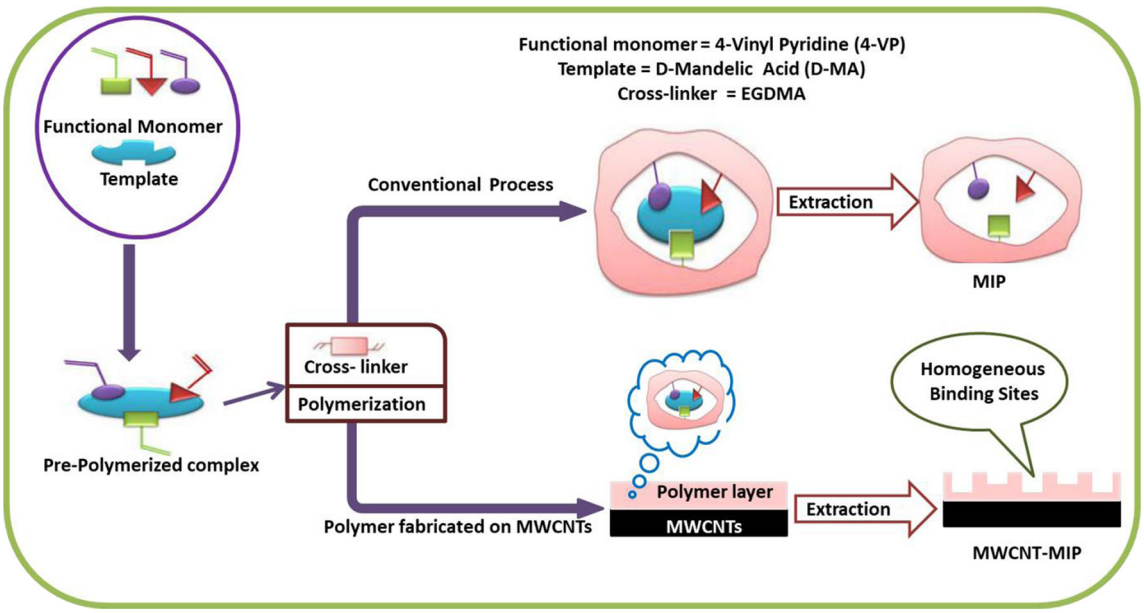

Scheme 3 Schematic representation of synthesis route of MIP & MWCNT-MIP

these different temperatures. For this, in a centrifuge tube, 10 mg of MWCNT-MIPs was suspended in 10 mL of D-MA with concentration 3.50 mmol L^{-1}. The tube was incubated at these different temperatures with shaking at different adsorption time intervals. The amount of D-MA adsorbed by MWCNT-MIPs was noticed by UV-vis spectrophotometer at 257.5 nm.

The sorption kinetics data of D-MA were analysed using the Langergen pseudo-second-order equation based on adsorption equilibrium capacity may be expressed in the form:

$$^{dQ_t}/_{d_t} = k_2(Q_e - Q_t)^2 \quad (3)$$

where k_2 is the rate constant of pseudo-second-order sorption. Integrating Eq. 3 and applying the initial conditions $Q_t = 0$ *at* $t = 0$ and $Q_t = Q_t$ *at* $t = t$,

$$^1/_{(Q_e - Q_t)} = {}^1/_{Q_e + k_2 t} \quad (4)$$

Or equivalently

$$^t/_{Q_t} = {}^1/_{k_2 Q_e^2} + {}^t/_{Q_e} \quad (5)$$

Thermodynamic studies

As commonly known, the enthalpy of adsorption is a thermal effect of the adsorption process, which is usually accompanying with the specific adsorption of the adsorbent and adsorbate and internal energy. The adsorption of MIPs is fundamentally the result of the induction of the template to the polymer. Hence, the change of adsorption enthalpy can indirectly define the inducement between MIPs and the template molecule. A larger adsorption enthalpy shows a stronger binding capacity of the MIPs to the template molecule. Though, the adsorption entropy is a function of the disordered state before and after adsorption, which reflects the change of adsorbate from the solution to the surface of the MIPs. Subsequently, according to the change of adsorption enthalpy and adsorption entropy, the adsorption process can be determined. Established on the thermodynamic theory, the correlation relationship of MIPs and NIPs are expressed as follows [34]

$$\ln\left(1 - \frac{Q_T x\, w}{n_0}\right) = \frac{\Delta H_{ad}}{RT} - \frac{\Delta S_{ad}}{R} \quad (6)$$

where n_0 is the initial molar number of the adsorbate; w is the mass of MIPs; ΔH_{ad} and ΔS_{ad} are the adsorption enthalpy and adsorption entropy, respectively; and T(K) is the absolute temperature of the adsorption process.

Adsorption isotherms

The adsorption isotherms play a vital role for the theoretical evaluation and interpretation of thermodynamic parameters [15]. It is used to characterise the interactions of each molecule with adsorbents. This provides a relationship between the concentration of the molecules in the solution and the amount of ion adsorbed on the solid phase when the two phases are at equilibrium [35]. In our systems considered, the Langmuir and Freundlichmodels were found to be applicable in interpreting D-MA adsorption on the D-MA-imprinted polymers such as MIP and MWCNT-MIP. The Langmuir isotherm is based on the assumption that: (a) the solid surface presents a finite number of identical sites which are energetically uniform; (b) there is no interaction between sorbed species, meaning that the amount of adsorbate molecules adsorbed has no influence on sorption rate; (c) monolayer is formed when the solid surface reaches saturation. The Langmuir adsorption isotherm is represented as follows,

$$Q_e = \frac{Q_m b C_e}{1 + C_e} \quad (7)$$

The above equation can be rearranged to the following linear form:

$$\frac{C_e}{Q_e} = \frac{C_e}{Q_m} + \frac{1}{bQ_m} \quad (8)$$

where C_e is the equilibrium concentration, Q_e the amount of D-MA adsorbed at equilibrium, Q_m is amount of D-MA adsorbed for a complete monolayer, b is a constant related to the energy or net enthalpy of sorption. The adsorption data were analyzed using the linear form, Eq. (8) of the Langmuir isotherm. The values for Q_m (from slope) and b (from intercept) can be obtained from the plots of specific sorption, C_e/Q_e, against the equilibrium concentration, C_e. The Freundlich expression is an exponential equation and therefore assumes that as the sorbate concentration increases, the concentration of sorbate on the adsorbent surface will increase.

Scheme 4 Chemical Structure of VMA, HVA and L-MA

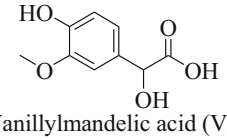

Vanillylmandelic acid (VMA)

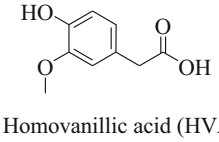

Homovanillic acid (HVA)

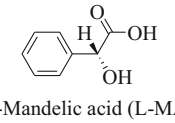

L-Mandelic acid (L-MA)

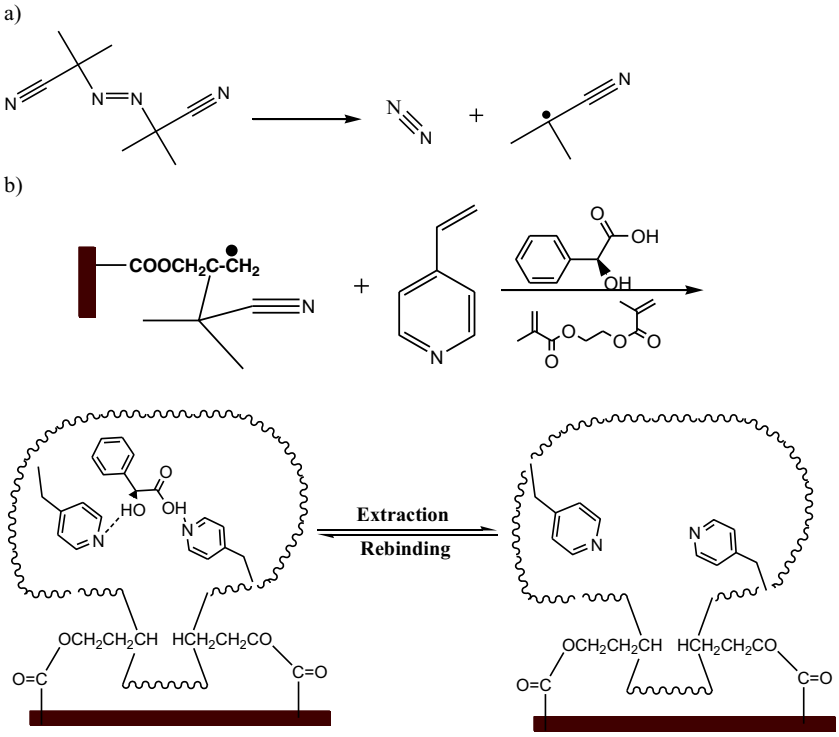

Scheme 5 Proposed mechanism for the synthesis of MWCNT-MIP [(**a**) Dissociation of AIBN, (**b**) Polymerization in the presence of pre-polymerized complex of D-MA and 4-VP with cross-linker EGDMA layered on MWCNTs followed by extraction of D-MA, which creates imprinted cavities of D-MA on polymer matrix]

$$Q_e = K_f C_e^{1/n} \tag{9}$$

The above equation is frequently used in the linear form by taking the logarithm of both sides as:

$$\log Q_e = log K_f + \frac{1}{n}\log C_e \tag{10}$$

where K_f and n are isotherm constants [36]. The applicability of the Freundlich adsorption is also analyzed by plotting log Q_e versus log C_e. From the plot we could determine the values of constants K_f and n. Langmuir and Freundlich isotherms were applied in both MWCNT-MIP and MIP and compared their results to find out the appropriate isotherm in our system.

Selectivity studies

For the selectivity studies, to the template desorbed polymer, equal volume of the solutions of template and the compound with structural analogues L-mandelic acid (L-MA), homovanillic

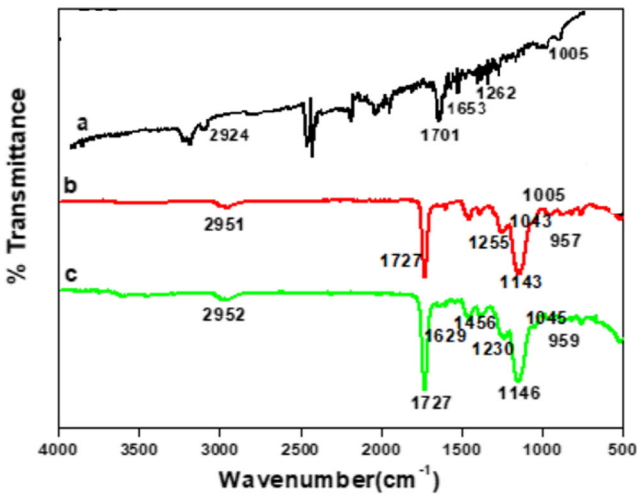

Fig. 1 FT-IR spectra of a) vinyl functionalized MWCNT, b) MIP and c) MWCNT-MIP

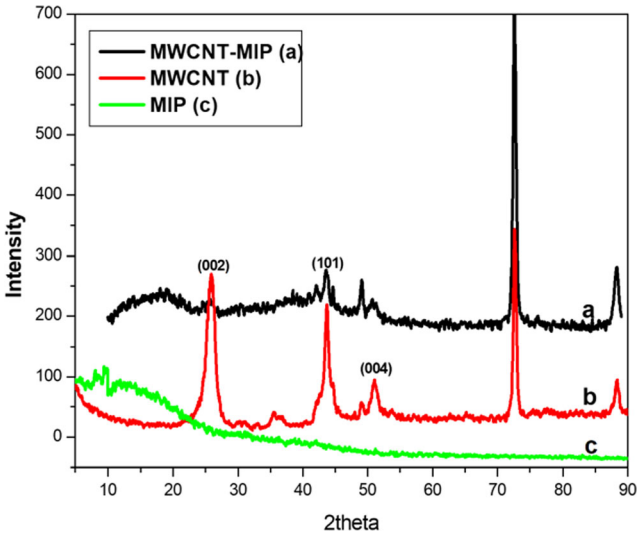

Fig. 2 X-ray diffractogram of a) MWCNT-MIP, b) MWCNT and c) MIP

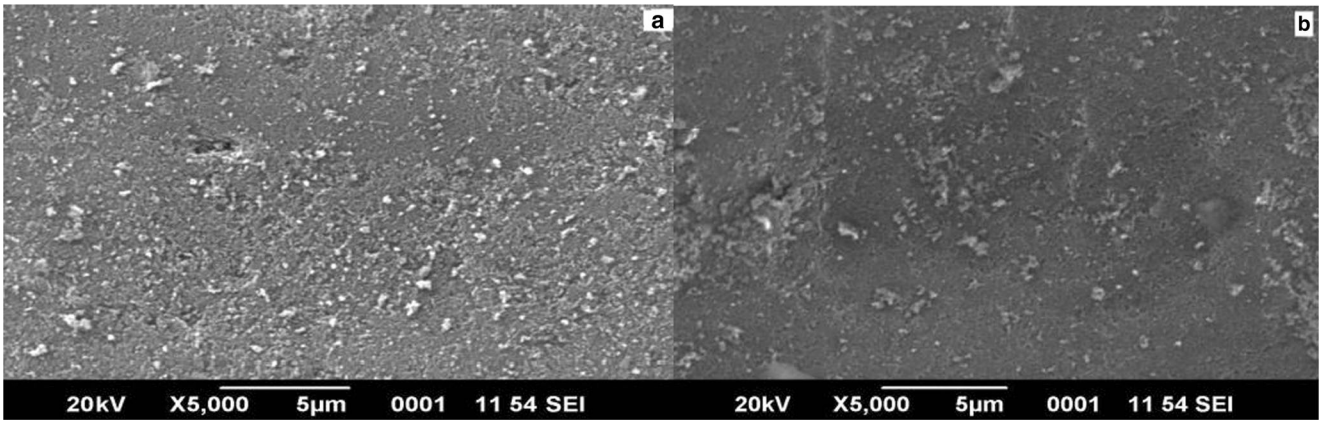

Fig. 3 SEM images of (**a**) MIP and (**b**) MWCNT-MIP

acid (HVA) and vanillylmandelic acid (VMA) having equal concentration were added in different tubes and the difference in the extent of binding was estimated spectrophotometrically. Scheme 4 depicted the structural similarity of selected analogues for selectivity studies. The imprinting factor or separation factor (α), which represents the effect of the imprinting process, is the ratio of the amount of substrate bound by the MIP to that bound by the corresponding NIP is determined using the enantiomer L-MA as the analogue [33].

Separation factor,

$$\alpha_{Template} = \frac{K_{MIP}}{K_{NIP}} \tag{11}$$

$$K = \frac{Template_{Bound}}{Template_{Free}} \tag{12}$$

The selectivity of the imprinted polymers towards the template was calculated in terms of selectivity factor (a).

Selectivity factor,

$$a = \frac{\alpha_{Template}}{\alpha_{Analogue}} \tag{13}$$

Reusability and robustness

The reusability capacity of MWCNT-MIP and MIP were determined in ten sequential cycles of adsorption-desorption technique. The extractions of D-MA from the polymer matrix in each cycle were carried out using the porogen acetonitrile.

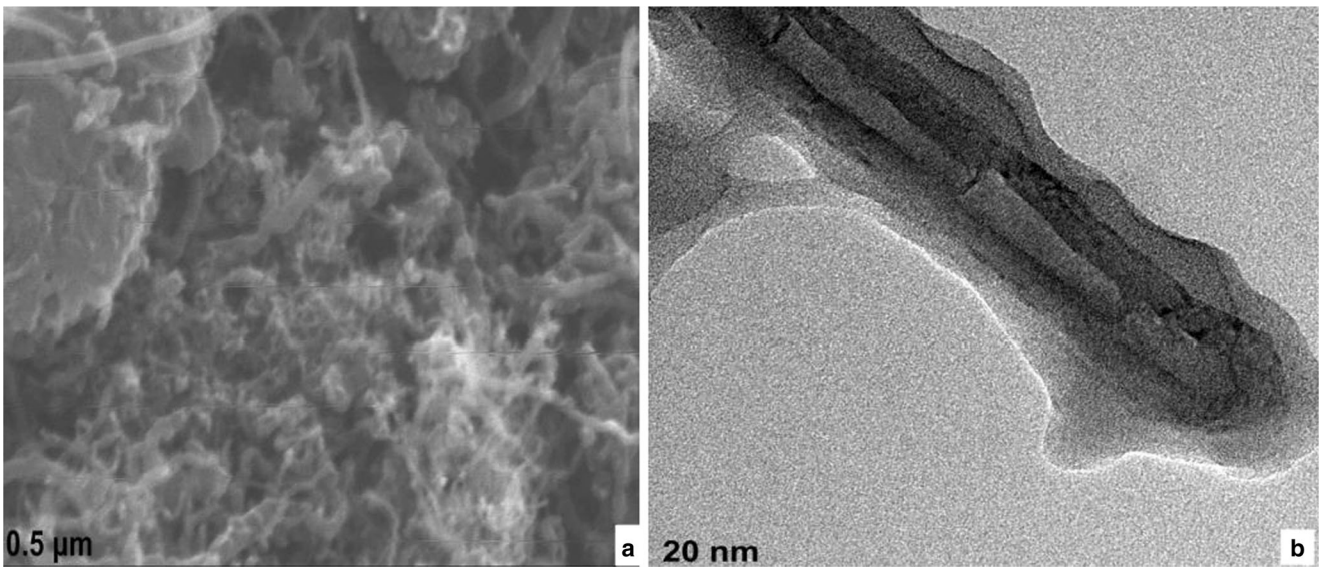

Fig. 4 TEM images of (**a**) MWCNT, and (**b**) MWCNT-MIP

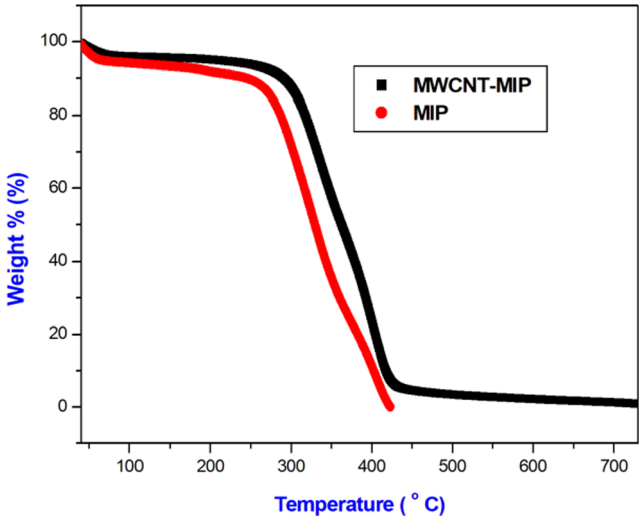

Fig. 5 Thermograms of a) MWCNT-MIP and b) MIP

Results and discussion

Vinyl group functionalized MWCNTs were used as a supporting material for the synthesis of MIPs with D-MA as the template molecule. Vinyl group functionalized MWCNT was prepared by three step processes includes conversion of pure MWCNT into MWCNT-COOH, conversion of carboxylic acid functionalized MWCNT to MWCNT-COCl and finally conversion of acyl chloride functionalized MWCNT to Vinyl-MWCNT. During this synthesis the carboxylic acid capacity of synthesised MWCNT-COOH was calculated as 3.05mmolg^{-1}. This value indicates the successful conversion of MWCNT to MWCNT-COOH with maximum acid capacity. The proposed mechanism of fabrication of imprinted cavity of D-MA layered on MWCNTs is depicted in Scheme 5.

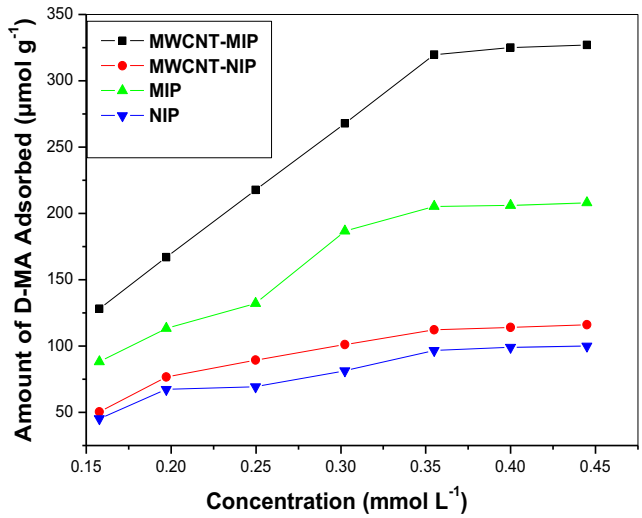

Fig. 6 Binding isotherm of MWCNT-MIP, MWCNT-NIP, MIP and NIP

Characterization of polymer particle

Ft-IR

The synthesis of MWCNT-MIP was primarily characterised by FT-IR spectroscopy evaluation. The FT-IR spectra of vinyl functionalised MWCNT, MIP and MWCNT-MIP are shown in Fig. 1.

The vibrational peaks corresponding to each spectrum are given below, a) 2924 cm^{-1} -C-H stretching, 1701 cm^{-1} -C=O stretching, 1653 cm^{-1} -C=C stretching, 1262 cm^{-1} -C-O symmetric stretching (ester), 1005 cm^{-1} out of plane C-H bending vibration b) 2951 cm^{-1} -C-H stretching, 1727 cm^{-1} -C=O stretching, 1043 cm^{-1} -C-N stretching, 1255 cm^{-1} -C-O symmetric stretching (ester), 1143 cm^{-1} -C-O asymmetric stretching (ester), 957 cm^{-1} -O-H Bending. c) 2952 cm^{-1} -C-H stretching,1727 cm^{-1} -C=O stretching, 1045 cm^{-1} -C-N stretching, 1230 cm^{-1} -C-O symmetric stretching (ester), 1146 cm^{-1} -C-O asymmetric stretching (ester), 959 cm^{-1} -O-H bending 1629 cm^{-1} -C=C Stretching, 1456 cm^{-1} -C-H deformation.

The vibrational peaks at 2924, 1701, 1653,1262 and 1005 cm^{-1} could be found in the spectrum (a) indicates the successful incorporation of vinyl group on the surface of MWCNT. The characteristic peaks of pure MIP were also appeared in the spectrum of MWCNT-MIP, which reveals the successful fabrication of MWCNT-MIP.

X-ray diffraction analysis

The X-ray diffraction technique was used to examine the crystalline nature of MWCNT-MIP. Figure 2 shows the X-ray diffraction patterns of MWCNT-MIP, MWCNT and MIP. The significant XRD patterns of the MWCNTs are appeared at 2θ of 25.3° and 43.6°, which is corresponding to the graphite (002) and (100) reflection planes of MWCNTs [JCPDS No: 01–0646]. The (002) reflection peak was observed at the same 2θ values in both MWCNT and MWCNT-MIP patterns. The intensity of diffraction peaks in MWCNT-MIP was decreased as compared to MWCNT. The conventional MIP scatter the X-ray beams to give a very broad peak (2θ = 5–20 °), which is characteristics of its amorphous nature. This is a good indication of successful fabrication of MIP layer on the surface of MWCNT. From XRD patterns, it can be concluded that the MWCNT is still had same cylinder wall structure and inter planar spacing after the attachment of MIP layer on it.The spatial extent of stacking of graphene layers is calculated using Scherrer's formula (L = 0.9 λ/B cosθ), where L is the mean size of the MWCNT-MIP particles, λ is the X-ray wavelength (Cu KR λKR1) 1.5418 Å), θ_{max} is the maximum angle of the (002) peak and $B(2\theta)$ is the half-peak width for MWCNT-MIP(002) in radians [37]. The value of L was found

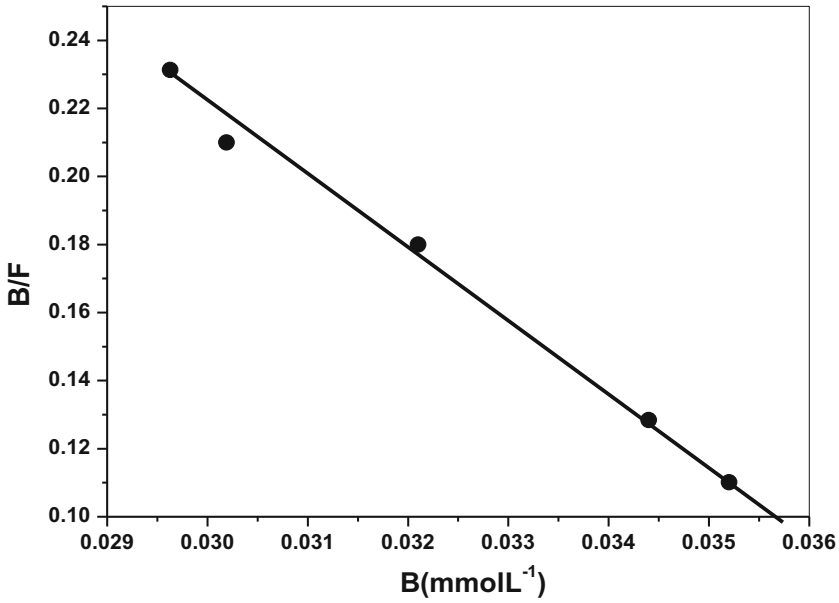

Fig. 7 Scatchard plot of D-MA on MWCNT-MIP

to be approximately 33 nm, which are in good agreement with TEM results.

Scanning Electron microscope analysis

The morphological characteristics of MWCNT-MIP and MIP were examined by SEM technique. In Fig. 3, MWCNT-MIP showed nanosized tubular moieties with an average size about 25–34 nm. Generally MIPs showed a rough surface morphology because of the extraction of template molecule from its polymer matrix. Here also the conventional MIPs displayed an agglomerated morphology which was significantly converted into tubular forms by the incorporation of MWCNT into the polymer matrix.

Transmission electron microscopy analysis

In order to know the detailed surface morphology, crude MWCNT and MWCNT-MIP were characterized with TEM. TEM micrographs of crude MWCNT before and after

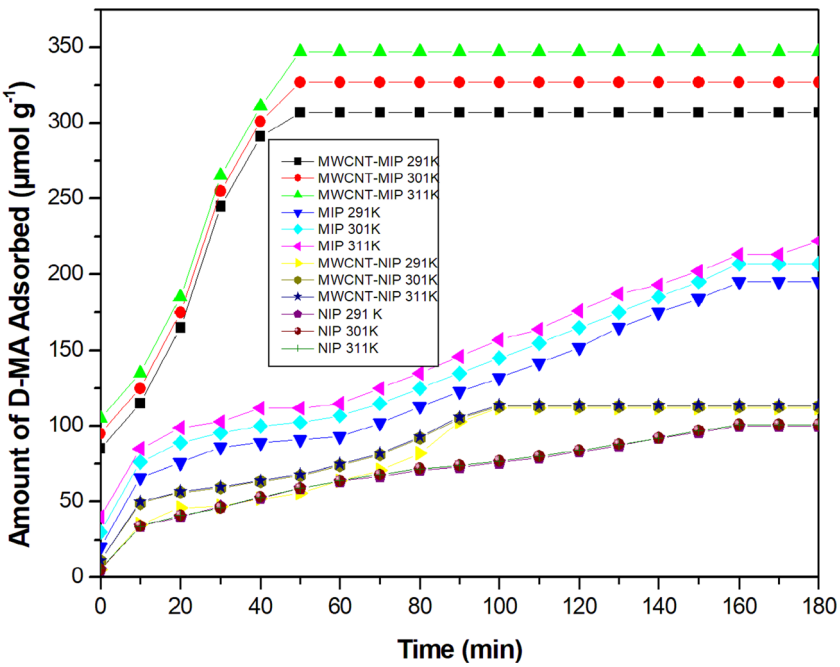

Fig. 8 The adsorption kinetics on MWCNT-MIP, MWCNT-NIP, MIP and NIP with different temperature

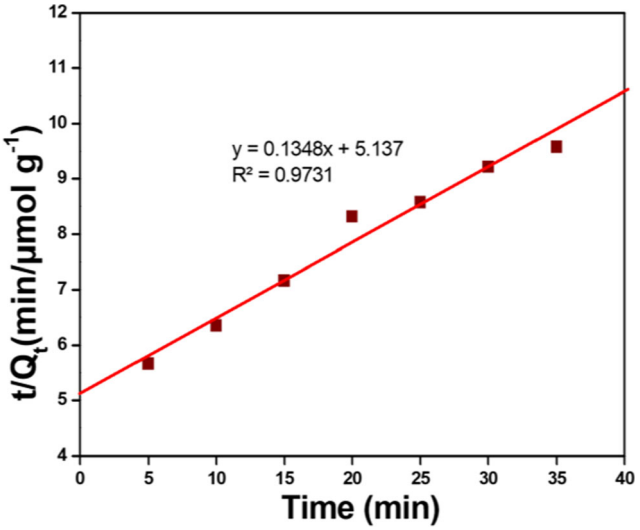

Fig. 9 Second order kinetics of the experimental data for MWCNT-MIP

fabrication of MIP are shown in Fig. 4. The image of MWCNT revealed that the crude multiwalled nanotubes are entangled with one another and formed a cross-linked structure due to the presence of impurities. Their average size was about 20 nm and the length was several micrometers. Compared to crude MWCNT, the outer wall thickness of MWCNT increased in MWCNT-MIP and also it preserved its nano fibrillar morphology. The average size was increased to 35 nm, which indicate the fact that an imprinted layer with thickness about 10–15 nm was successfully wrapped around the vinyl functionalized MWCNT.

Thermogravimetric analysis (TGA)

Thermogravimetric analysis was carried out to investigate the thermal stability of MWCNT-MIP and MIP which is depicted in Fig. 5.The nature of thermograms of both MWCNT-MIP and MIP showed similar pattern. In comparison with MWCNT-MIP, conventional MIP revealed a lower decomposition temperature and higher weight loss. Conventional MIP started its decomposition at 242 °C and became completely dissociated at 423 °C, whereas MWCNT-MIP started its decomposition at around a temperature of 341 °C. These factors suggested that MWCNT-MIP possess better thermal stability due to the incorporation of MWCNTs.

Adsorption experiments

In order to observe the binding performance of the surface imprinted MWCNT-MIP against control MWCNT-NIP, an equilibrium binding analysis was carried out. Hydrogen bonding and π-π, interactions are the major interactions between the functional monomer 4-VP and template molecule D-MA. The binding isotherm depicted a saturation curve which indicate that a finite number of binding sites exist in the imprinted polymer. As shown in Fig. 6, the adsorption capacity of MWCNT-MIP was much higher than that of MIP. This revealed that MWCNT-MIP has a distinctive capacity for D-MA, which could be attributed to the complementary cavities formed in the MWCNT-MIP materials. The surface-imprinted MWCNT-MIP has a higher binding capacity than that of the MWCNT-NIP. The weak adsorption of D-MA to the MWCNT-NIP may be attributed to non-specific interaction with the polymer matrix.

Scatchard analysis of the binding of D-MA to MWCNT-MIP

The data obtained from adsorption experiment was further processed with the Scatchard equation to measure the binding

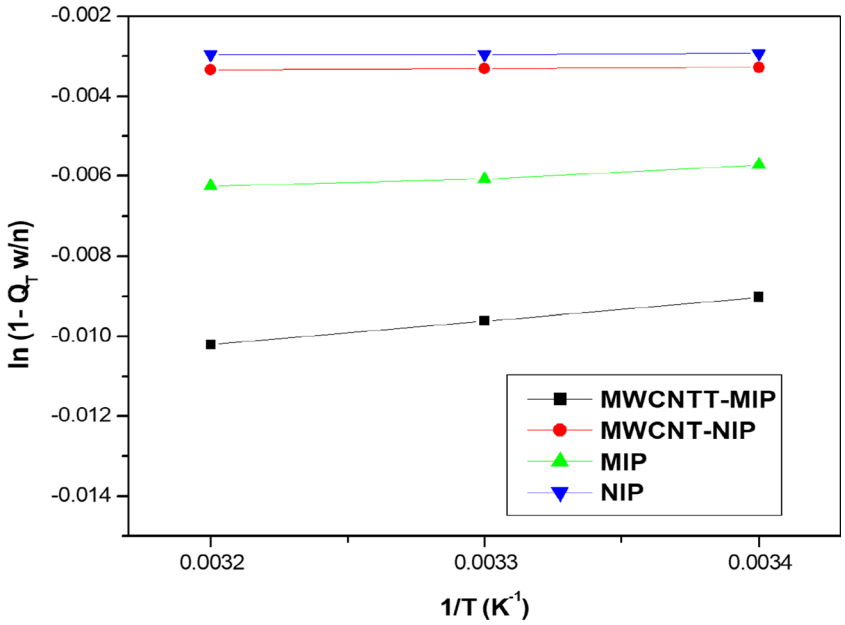

Fig. 10 Thermodynamically correlating the relative adsorption of D-MA

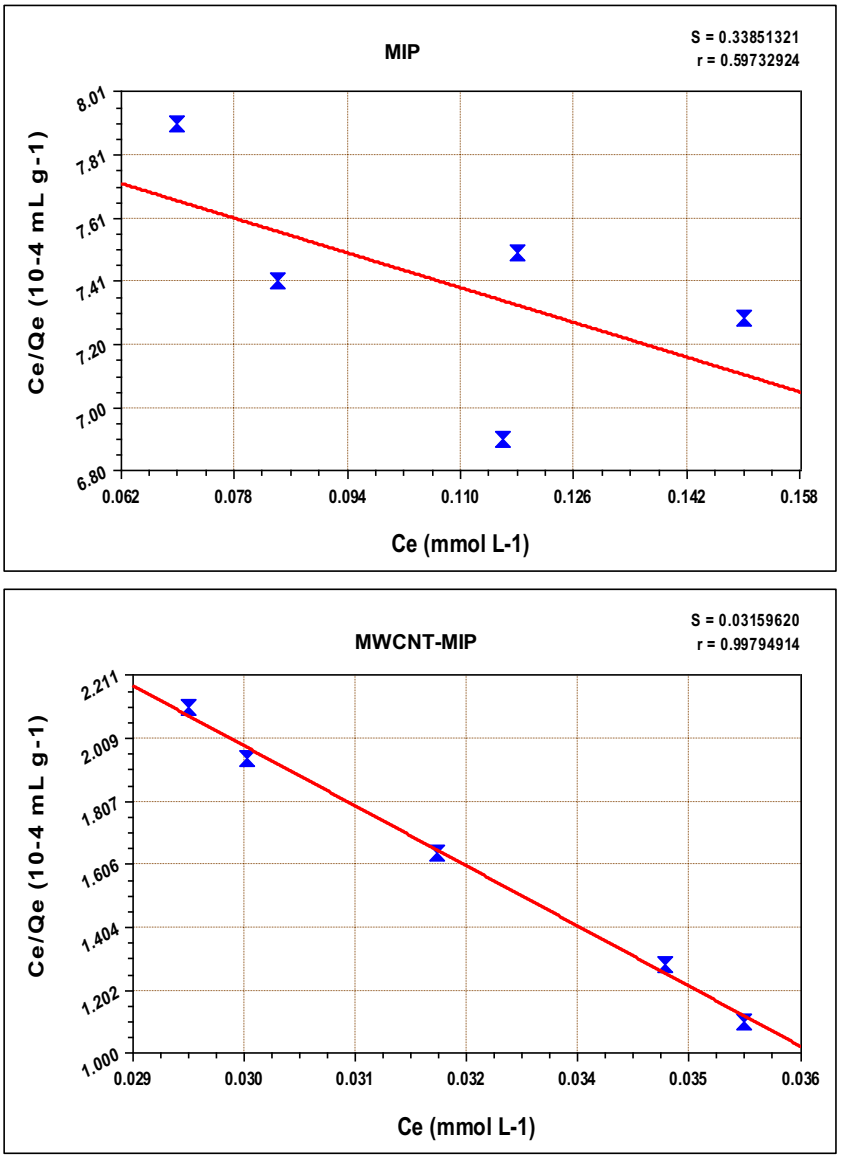

Fig. 11 Langmuir isotherms of MIP and MWCNT-MIP

parameters of the MWCNT-MIP. Scatchard plot was constructed by plotting the ratios of bound amount to free D-MA concentration against the bound concentration. As shown in Fig. 7, one straight line fit the scatchard equation, $B/F = (B_{max}-B)/K_d$, and it gave two typical binding parameters. The equilibrium dissociation constant K_d is 21.01 mmol $L^{-1}$and the maximum number of binding sites B_{max} is (5 mmol g^{-1}).

Adsorption dynamics and kinetics

Figure 8 shows the time dependence of the adsorption capacities of D-MA towards imprinted polymer as a function of time with three different temperatures. It revealed that the amount of adsorption increased with an increase in temperature or adsorption time. As shown, D-MA adsorption initially increased and then increased slowly with the time extension. In the case of MWCNT-MIPs, after 50 min the adsorption process reached equilibrium, whereas in MIPs, it happened only at 160 min. This is probably due to high complexation between D-MA molecules and D-MA cavities in the imprint polymer structure. At the initial stage a large number of imprinted cavities existed on the support, so D-MA molecule was easy to reach the specific binding sites. When the recognition cavities were filled up, the rate of adsorption dropped significantly and then the adsorption process achieved equilibrium. The increased adsorption rate also implies that the imprinted cavities situated in the surface which make the recognition cavities accessible for the template molecule and hence take shorter time to reach adsorption equilibrium.

The plot of t/Q_t against t, which given in Fig. 9, has high correlation coefficient (0.9731) which revealed that the D-MA adsorption using MWCNT-MIP is in good agreement

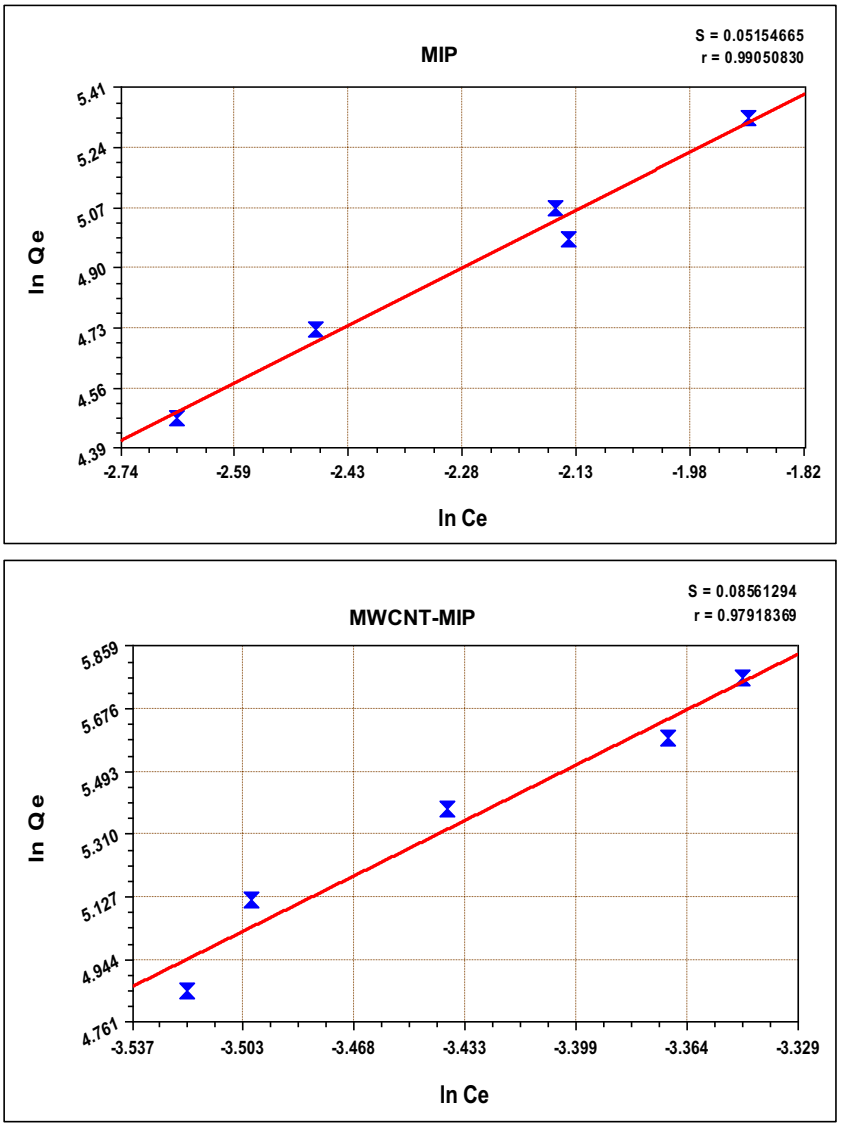

Fig. 12 Freundlich adsorption isotherms of MIP and MWCNT-MIP

with the second order kinetics reaction with rate constant $k_2 = 0.1482$ mol^1 min^{-1}.

Thermodynamic studies

Based on Eq. (6), the plot of ln(1 - Q_T w/n) vs. (1/T) is shown in Fig. 10 in which the plots are normally expected to be a straight line. Compared with NIPs, the MIPs showed a significantly different adsorption behavior for D-MA. Relative to NIPs (for MWCNT-NIP, $\Delta H_{ad} = 15.128$ KJmol^{-1}and for NIP = 12.471KJmol^{-1}), the adsorption enthalpy of MIPs was obviously larger (for MWCNT-MIPs, $\Delta H_{ad} = 49.0526$ KJmol^{-1} and for MIP $\Delta H_{ad} = 22.0321$KJmol^{-1}). This indicates that the inducement of MIPs for D-MA is greater than that of NIPs. Among MWCNT-MIP and MIPs, polymer formed on nanotubes shows greater enthalpy value which will again enhance the inducement of polymer for D-MA. Conversely, the adsorption entropy of MIPs (for MWCNT-

Table 1 Adsorption isotherm parameters of MIP and MWCNT-MIP

Sample	Langmuir parameters			Freundlich parameters		
	Q_m (μmol g^{-1})	b (Lmmol^{-1})	R	N	K_f [(mmol/g)(L/mmol)$^{1/n}$]	r
MIP	75.19	0.2398	0.5973	0.9389	1527.519	0.9905
MWCNT-MIP	315.23	0.5814	0.9979	0.2145	136.6155	0.9792

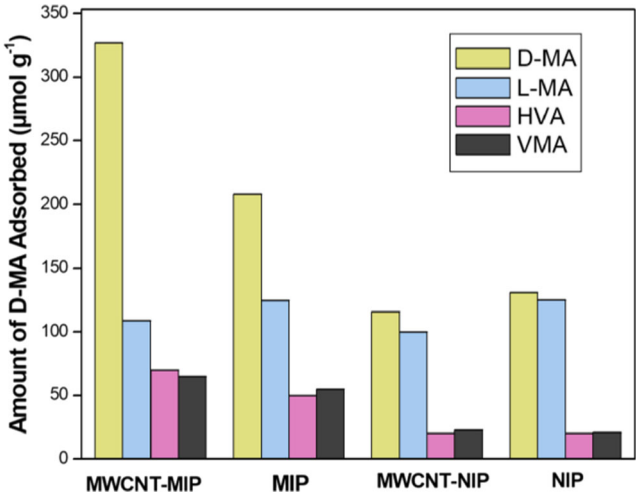

Fig. 13 Evaluation of selectivity of the D-MA imprinted polymer

MIP, $\Delta S_{ad} = 24.177$ KJ mol^{-1} K^{-1} and for MIPs, $\Delta S_{ad} =$ 12.2698 KJ mol^{-1} K^{-1}) was less than NIPs (for MWCNT-NIP, $\Delta S_{ad} = 27.829$ KJ mol^{-1} K^{-1} for NIP, $\Delta S_{ad} = 28.6417$ KJ mol^{-1} K^{-1}).The change in adsorption entropy, which reveals a difference in the adsorption behaviour of polymer fabricated on MWCNTs and on conventional polymer matrix, may be the result of the increased interaction between the molecules due to the high specific imprint. According to the results of the adsorption isotherms and kinetics, D-MA adsorption on MWCNT-MIP was the spontaneous process of enthalpy control.

Adsorption isotherms

During the adsorption experiments, adsorption isotherms were used to evaluate adsorption properties. The sorption data were analysed using the linear form of the Langmuir isotherm and Freundlich isotherm. All the calculations of adsorption isotherms were performed by Curve Expert- Version 1.4 software. This program uses non-linear least square fitting of the averaged experimental data by using the Marquardt-Levemberg algorithm [38]. In Langmuir isotherm, the plots of specific sorption, C_e/Q_e, against the equilibrium concentration, C_e, for MWCNT-MIP polymer and MIP were plotted which is depicted in Fig. 11.

From the above curve of Langmuir isotherms, correlation coefficient (r) of MWCNT-MIP is found to be 0.9979. Here adsorption isotherm data provided the information that the adsorption process was mainly monolayer on a homogeneous adsorbent surface. The Langmuir constants Q_m and b were found to be 315.23 µmol g^{-1}and0.5814 Lmmol^{-1}, respectively. It is also exciting to note that the D-MA adsorption capacity calculated from Langmuir equation (315. 23 µmol g^{-1}) is closely associated with that of experimental data (317.87 µmol g^{-1}) which was achieved from the concentration study.

Freundlich adsorption isotherm was analysed by plotting log Q_e versus log C_e for MWCNT-MIP polymer and MIP which is depicted in Fig. 12.

Freundlich adsorption isotherm is an empirical one for non-ideal adsorption on heterogeneous surfaces. In the case of MWCNT-MIP the theoretical and experimental values of the Freundlich isotherm show an enormous deviation whereas the Langmuir isotherm do not. Consequently it can be determined that the Langmuir isotherm model was more suitable for the experimental data of MWCNT- -MIP than Freundlich isotherm. Langmuir and Freundlich adsorption isotherm parameters of both the MIP and MWCNT-MIP were shown in Table 1. D-MA adsorption in MWCNT-MIP takes place at specific homogeneous sites and no further adsorption takes place at the site which has already been bounded by a template molecule. The well fit curve of Freundlich model obtained for MIP indicated the heterogeneity of the bulk imprinted polymer.

Selectivity of the D-MA imprinted polymer

The chiral recognition ability of synthesized MWCNT-MIP on D-MA was estimated using its enantiomer L-MA, HVA and VMA. The concentration of D and L enantiomers, and these structurally related compounds were chosen as 0.3418 mmolL^{-1}, which is the maximum adsorption concentration of D-MA revealed from binding analysis. Figure 13 revealed that the non-imprinted polymer prepared without the template molecule were not able to recognize the chirality. This is because of the production of non-specific binding sites in the polymer matrix. The maximum adsorption quantity of synthesised MWCNT-MIP towards D-MA and L-MA is about 356 and 109 µmolg^{-1} respectively. This result demonstrates that the interaction between the functional monomer and the template should have a crucial effect for creating the adsorption sites. The shape or sites constructed on the polymer

Table 2 Selectivity factor of the polymer

	Separation factor of D-MA	Separation factor of L-MA	Selectivity factor, $a = \frac{\alpha_{Template}}{\alpha_{Analogue}}$
$\alpha_{Template} = \frac{K_{MWCNT-MIP}}{K_{MWCNT-NIP}}$	6.0396	1.0285	5.8720
$\alpha_{Template} = \frac{K_{MIP}}{K_{NIP}}$	2.2981	1.0084	2.2789

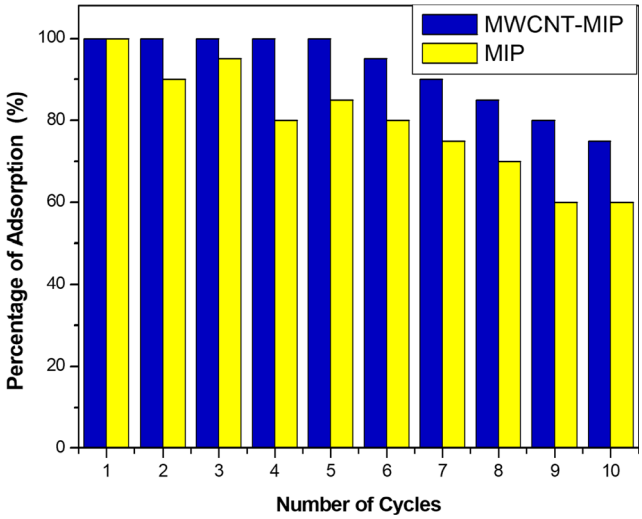

Fig. 14 Adsorption-desorption cycles of MWCNT-MIP and MIP

surface were complementary to the imprinted D-MA should have a vital role to recognize the molecular chirality.

From Table 2, it revealed that MWCNT imprinted polymer have high selectivity factor towards target molecule than conventional MIP. This indicates the homogenous binding site formation on surface of MWCNT. Large number of template recognition cavities was formed in the surface of MWCNT-MIP and it shows high binding towards the D-MA molecule. The high specificity is mainly attributed to the unique binding of the imprinted sites to the target molecule, so they cannot bind the other analogues tightly.

Reusability and robustness

Figure 14 shows the adsorption efficacy of MWCNT-MIP and MIP in ten consecutive adsorption-desorption cycles. The results revealed that the MWCNT-MIP showed 100% adsorption regeneration upto five cycles. The regeneration efficiency then lowered due to the damage of some recognition sites in MWCNT-MIP matrix during the extraction process and hence not fit for further adsorption of D-MA molecule. The conventional MIP showed unequal trends of regeneration from the second cycle onwards due to the destruction of binding sites and also difficulties in leaching out the entire D-MA from the bulk polymer matrix during its extraction period. Hence it is confirmed that MWCNT-MIP exhibits the properties of a better adsorbent of D-MA than the conventional MIP.

Conclusions

A novel sorbent for enantioselective recognition for D-MA is successfully fabricated on vinyl functionalized MWCNT via molecular imprinting approach. The complementary nature of the template and functional monomer were obtained in the pre-polymerized complex studies. The results of the high adsorption amount MWCNT-MIP particles for D-MA adsorption suggest that the nanolayer MIP preparation on the surface of the MWCNTs could improve the porous site availability compared to bulk polymerization. FT-IR spectroscopy, TEM, SEM and XRD confirmed the homogeneous formation of MWCNT-MIP binding sites. The homogeneity was again confirmed by Langmuir adsorption isotherm. The stability of MWCNT-MIP was upto425 ^{o}C. The adsorption kinetics of D-MA on MWCNT-MIP was in agreement with the second-order rate equation. The high separation factor suggest that non-covalent molecular imprinting with MWCNTs as supporting material is a promising method for analyzing chiral compound with a simple structure.

References

1. Chemie O, Bonn BDU, Sarhan A (1977) Enzyme-analogue built polymers. Makromol Chem 178:2799–2816
2. Fonseca Silva C, Bastos Borges K, Soares do Nascimento Jr C (2018) Rational Design of a Molecularly Imprinted Polymer for Dinotefuran: theoretical and experimental studies aimed at the development of an efficient adsorbent for microextraction by packed sorbent. Analyst 143:141–149
3. Hosoya K, Shirasu Y, Kimata K, Tanaka N (1998) Molecularly imprinted chiral stationary phase prepared with racemic template. Anal Chem Acta 70(5):943–945
4. Ou J, Dong J, Tian T, Hu J, Ye M, Zou H (2007) Enantioseparation of Tetrahydropalmatine and Tröger ' s base by molecularly imprinted monolith in capillary Electrochromatography. J Biochem Biophys Methods 70:71–76
5. Lu Y, Li C, Zhang H, Liu X (2003) Study on the mechanism of chiral recognition with molecularly imprinted polymers. Anal Chim Acta 489(489):33–43
6. Yoshida M, Hatate Y, Uezu K, Goto M (2000) Chiral-recognition polymer prepared by surface molecular imprinting technique. Colloids Surf A Physicochem Eng Asp 169:259–269
7. Lingxin S, Wang X, Lu W, Wu X, Li J (2016) Molecular imprinting : perspectives and applications. Chem Soc Rev 45:2137–2211
8. Chianella I, Karim K, Piletska EV, Preston C, Piletsky SA (2006) Computational design and synthesis of molecularly imprinted polymers with high binding capacity for pharmaceutical applications-model case: adsorbent for Abacavir. Anal Chim Acta 559(1):73–78
9. Karim K, Breton F, Rouillon R, Piletska EV, Guerreiro A, Chianella I, Piletsky SA (2005) How to find effective functional monomers for effective molecularly imprinted polymers? Adv Drug Deliv Rev 57(12):1795–1808
10. Spivak DA (2005) Optimization , evaluation , and characterization of molecularly imprinted polymers B. Adv Drug Deliv Rev 57: 1779–1794
11. Fu Y, Chen Q, Zhou J, Han Q, Wang Y (2012) Enantioselective recognition of Mandelic acid based on c -globulin modified glassy carbon electrode. Anal Biochem 421(1):103–107
12. Hwang C (2005) Molecular recognition properties of mandelic acid by using molecularly imprinted polymer. J Appl Polym Sci
13. Bai L, Chen X, Huang Y (2013) Chiral separation of racemic Mandelic acids by use of an ionic liquid-mediated imprinted monolith with a metal ion as self-assembly pivot. Anal Bioanal Chem 405:8935–8943

14. Zhou J, Liu Q, Fu G, Zhang Z (2013) Separation of Mandelic acid and its derivatives with new immobilized cellulose chiral stationary phase. Zhou al. / J Zhejiang Univ-Sci B (Biomed Biotechnol) Press J. Zhejiang Univ. B (Biomedicine Biotechnol. 1–6
15. Mao S, Zhang Y, Rohani S, Ray AK (2012) Chromatographic Resolution and Isotherm Determination of (R , S) -Mandelic Acid on Chiralcel-OD Column. 2273–2281
16. Kan X, Zhao Y, Geng Z, Wang Z, Zhu J (2008) Composites of multiwalled carbon nanotubes and molecularly imprinted polymers for dopamine recognition. J Phys Chem C 112:4849–4854
17. Xu L, Xu Z (2012) Molecularly imprinted polymer based on multiwalled carbon nanotubes for ribavirin recognition. J Polym Res 19:1–6
18. Rezaei B, Rahmanian O (2012) Direct Nanolayer preparation of molecularly imprinted polymers immobilized on multiwalled carbon nanotubes as a surface-recognition sites and their characterization. J Appl Polym Sci 125:798–803
19. Scida K, Stege PW, Haby G, Messina GA, García CD (2011) Recent applications of carbon-based nanomaterials in analytical chemistry : critical review. Anal Chim Acta 691(1–2):6–17
20. Wang S (2009) Optimum degree of functionalization for carbon nanotubes. Curr Appl Phys 9(5):1146–1150
21. Wackerlig J, Schirhagl R Applications of molecularly imprinted polymer nanoparticles and their advances toward industrial use: a review. Anal Chem 88:250–261
22. Meng L, Fu C, Lu Q (2009) Advanced technology for functionalization of carbon nanotubes. Prog Nat Sci 19(7):801–810
23. Han Z, Fina A (2011) Progress in polymer science thermal conductivity of carbon nanotubes and their polymer nanocomposites : a review. Prog Polym Sci 36(7):914–944
24. Zhang X, Zhang Y, Yin X, Du B, Zheng C, Yang HA (2013) Facile approach for preparation of molecularly imprinted polymers layer on the surface of carbon nanotubes. Talanta 105:403–408
25. Hone J (2004) Carbon nanotubes : thermal properties. Dekker Encycl Nanosci Nanotechnolog:603–611
26. Senger RT (2004) Functionalized carbon nanotubes and device applications. J Phys Condens MATTER 16:901–960
27. Valle M, Pumera M, Llopis X, Pe B (2005) New materials for electrochemical sensing VI : carbon nanotubes. Trends Anal Chem 24(9):826–838
28. Belin T, Epron F (2005) Characterization methods of carbon nanotubes : a review. Mater Sci Eng B 119:105–118
29. Iijima S (2006) Carbon nanotubes. Electrochem Soc Interface:23–26
30. Yang W, Thordarson P, Gooding JJ, Ringer SP, Braet F (2007) Carbon nanotubes for biological and biomedical applications. Nanotechnology 18:412001
31. Xu L, Xu Z (2012) Molecularly imprinted polymer based on multiwalled carbon nanotubes for ribavirin recognition. J Polym Res 19(8):9942
32. Rosca ID (2005) Oxidation of multiwalled carbon nanotubes by nitric acid. Carbon N Y 43:3124–3131
33. Polimer P, Molekul C (2010) Synthesis and characterization of a molecularly imprinted polymer for Pb 2 + uptake using 2-Vinylpyridine as the complexing monomer. Sains Malaysiana 39(5):829–835
34. Zhang W, Li Q, Cong J, Wei B, Wang S (2018) Mechanism analysis of selective adsorption and specific recognition by molecularly imprinted polymers of Ginsenoside Re. Polymers (Basel) 10(216)
35. Zhang H, Zhang Z, Hu Y, Yang X, Yao S (2011) Synthesis of a novel composite imprinted material based on multiwalled carbon nanotubes as a selective melamine absorbent. J Agric Food Chem 59:1063–1071
36. Zakaria ND, Yusof NA, Haron J, Abdullah AH (2009) Synthesis and evaluation of a molecularly imprinted polymer. Int J Mol Sci 10(1):354–365
37. Mahanandia P, Vishwakarma PN, Nanda KK, Prasad V (2006) Multiwall carbon nanotubes from pyrolysis of tetrahydrofuran. Mater Res Bull 41(41):2311–2317
38. Panahi R, Vasheghani-farahani E, Shojaosadati SA (2008) Determination of adsorption isother for L-lysine imprinted polymer. Iran J Chem Eng Chem Eng 5(4)